# CHAPTER IV
# EXPERIMENT AND RESULTS

This chapter describes the setup of equipment and apparatus used in the experiment. The experimental procedure is designed and conducted to investigate the optimization searching method of energy resolution in comparison with conventional experimentation in nuclear spectroscopy system. The experimental task consists of two major parts: input parameter preparation for simulation and optimization searching method.

## 4.1 Experiment apparatus

A set of electronic instrument, nuclear instruments and computer soft wares are employed for input parameters preparation and signal simulation. The system comprises of:

### 4.1.1 Electronic instrument:

A. Digital storage oscilloscope: Tektronix model TDS 360

B. Function generator: Hewlett Packard model 8111A

C. Personal computer with Pentium 4 processor or higher, on board memory at least 256 MB RAM and RS-232 communication port, operated under windows XP system program.

### 4.1.2 Application softwares:

A. MATLAB programs version 6.5 with signal processing toolbox.

B. Developed programs for digital filter design.

### 4.1.3 Nuclear instrument:

A. NIM Bin with power supply: ORTEC 4001C

B. Pulser: CANBERRA model 807

C. Spectroscopy amplifier: CANBERRA model 2022

D. Multichannel analyzer: CANBERRA model 35 plus

E. CdTe Detector-preamplifier: AMPTEK model XTR100

F. 5 mCi Am-241 radioisotope source with collimator

G. Cables and connector accessories.

## 4.2 Experimental procedure

### 4.2.1 Input parameter preparation for simulation

#### 4.2.1.1 Front-end signal generation

**4.2.1.1.1 Noise simulation.** The experimental equipment consists of AMPTEK XTR100 CdTe low energy x-ray detector with preamplifier and high voltage biasing, Tektronix digital oscilloscope model TDS 360 and personal computer which is used to control the data acquisition and data calculation, in collaboration with the MATLAB programs. Fig.4.1 shows the diagram of experimental system. The system is set under an operating condition with low background environment and keeping a warm up time for half an hour to ensure their system stability. For data acquisition, the signal containing noise and very little background generated by preamplifier's devices and CdTe radiation detector is digitized by digital oscilloscope. A thousand of sampled noise has been sent to the computer via the serial port of digital oscilloscope for performing a calculation of the mean, standard deviation, root-mean square, amplitude distribution and power spectral density.



Detector and high voltage     Preamplifier     Digital Oscilloscope     Computer
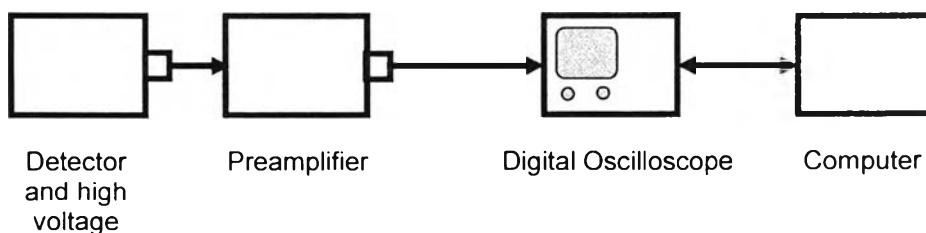
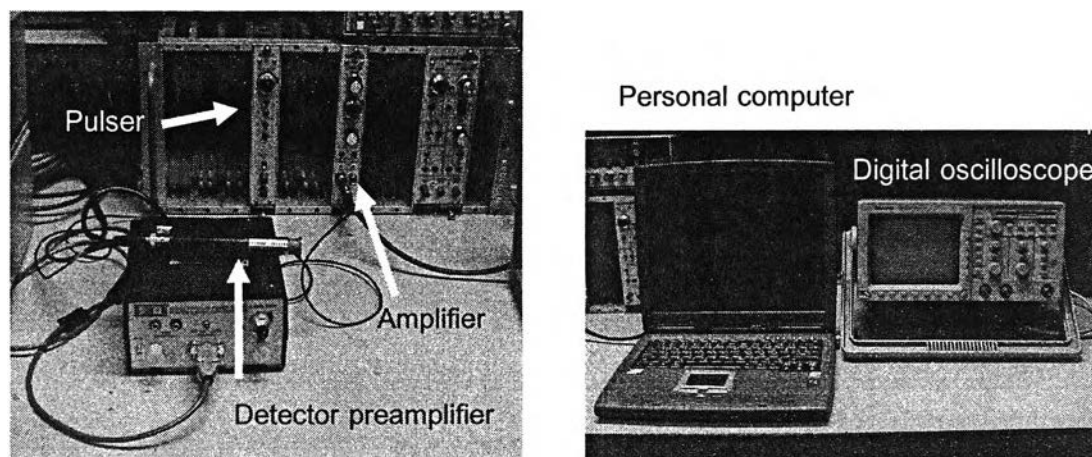Fig. 4.1 The system set-up for sampling a sequence of noise from preamplifier.

Fig. 4.2 Photograph of spectroscopy system set-up for sampling a sequence of noise from preamplifier output.

In computational process, the empirical cumulative distribution function of noise amplitude is calculated by *ecdf* function in MATLAB. This function is applied to calculate the Kaplan-Meier estimate of the cumulative distribution function (cdf), also known as the empirical cumulative distribution function of the sequence of noise samples. The calculated empirical distribution function of a sequence of noise samples is shown in Fig. 4.3. The criterion of using this function is the input of the large number of samples and in this case the ample size of sampled signals ensures that the criteria requirement is met.
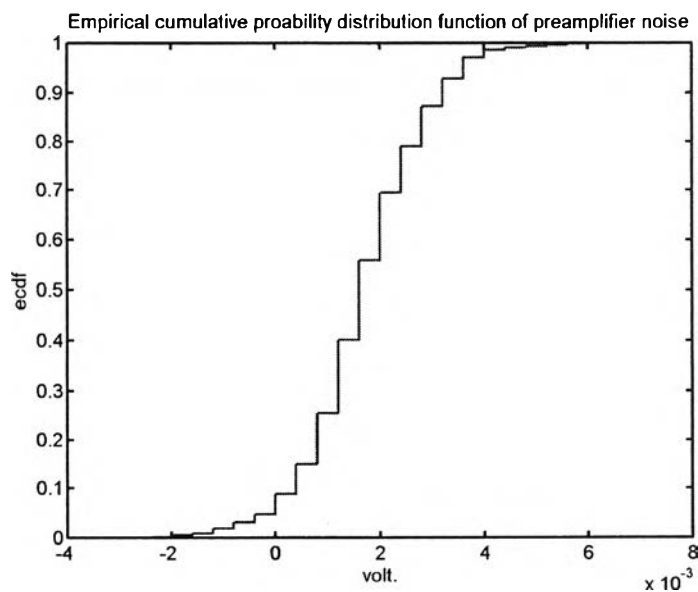


Fig. 4.3 Calculated empirical distribution function of a sequence of noise sample.

To simulate noise that has the same characteristic in frequency and time domain of preamplifier output under test, the data must be created from random number of a known distribution function. The method used to generate random number is the Inverse Function method, which is the popular method in Monte Carlo simulation. The benefit of this method is the usage of the observed data themselves to specify a data distribution directly. Signal samples are drawn during the simulation, rather than fitting a theoretical distribution to data. The simulated noise signals of preamplifier output are regenerated as shown in Fig. 4.4b.

4.2.1.1.2 Random photon signal generation. An input parameter to be used to simulate the exponential decay pulse of preamplifier output which carries the random emission rate of photon radiation (disintegration of radioisotope) and an energy magnitude can be established by combining two equations of Eq. (3.6 ) and Eq. (3.7), with an insertion of known parameters such as mean count rate and pulse decay time constant. In this case the time interval distribution ($\Delta t$) of radioisotope decay is obtained from uniform random numbers from 0 to 1 and mean count rate at 50 cps from puiser, 60 cps and 1000 cps from radiation count rate, respectively and they account for the input to equation (4.1)

$$\Delta t = \frac{\log(1 - \text{random number })}{- \text{mean count rate}} \tag{4.1}$$

Preamplifier output signal ($V_d$) simulation can be obtained from equation:

$$V_d = Ae^{-t/\tau} \tag{4.2}$$

Term A is arbitrary value corresponding to energy deposited within detector and $\tau$ is pulse decay time of the preamplifier, typically use at 50 µs. The simulation start from t=0 and proceeds until time equal to the time interval which is drawn from equation 4.1. The new pulse will be generated and randomly superimposes on a trailing edge of previous pulse. This means that the present and previous signals can be added together becoming a consecutive pulse. The simulated pulse with 50 µs decay time at constant amplitude under $\Delta t$ function is shown in Fig. 4.4, and the simulated pulse at a constant rate and amplitude stands for pulser output.

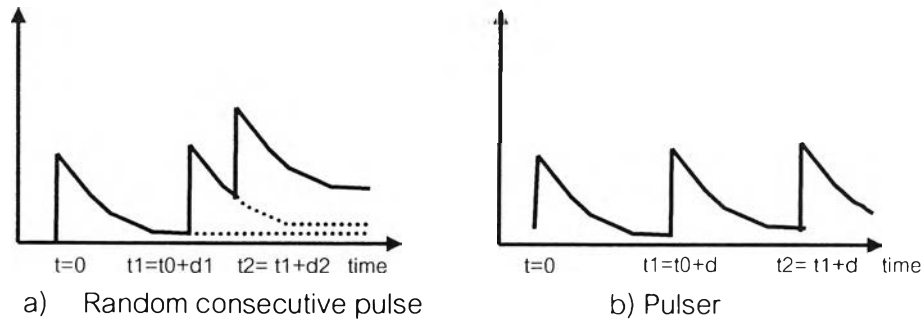a)    Random consecutive pulse                    b) Pulser

Fig. 4.4 Illustrated pulse of preamplifier pulse output at constant amplitude.

The front-end signal in time domain generation can be achieved by adding a simulated noise to a simulated pulse of preamplifier output, for using as signal input function.

### 4.2.1.2 Spectroscopy amplifier transfer function estimation

**4.2.1.2.1 Frequency response estimation.** The experimental equipment consists of CANBERRA 2022 spectroscopy amplifier, Hewlett Packard 8111A function generator, TDS 360 Tektronix digital oscilloscope and personal computer which is used to control the data acquisition and to establish the data calculation under MATLAB script command program. Fig. 4.5 shows the setup diagram of the experimental system. The system is set under low noise environment and keeping a warm up time for half an hour for ensures their system stability. A rectangular pulse a 16 ms pulse width ($t_w$),   60  mV magnitude and 9 Hz pulse rate generated from the function generator, is applied to a spectroscopy amplifier input with  gain setting of 96 (CG=300, FG=0.32). Only front step of rectangular pulse, at time t< $t_w$, acquire by digital oscilloscope acts as a step-voltage input. Both of step input and response output signals of spectroscopy amplifier at a shaping time varying from 0.5,1.0, 2.0, 4.0, 8.0 and 12 µs, are digitized by 5 MHz sampling frequency at 0.2 µs sampling interval. A thousand sampled signals of each shaping time are sent to the computer via a serial port, set by set, for performing calculations of input and output power spectral density. The frequency response transfer function of a filter in spectroscopy amplifier is simply reconstructed by dividing the cross power spectral of step input of amplifier output by auto power spectrum of step input, as in equation 2.10 . Welch's method based on

Fourier transform in "tfe" MATLAB script command is used to estimate the function. All frequency response of spectroscopy amplifier at each shaping time is shown in Fig. 4.13.
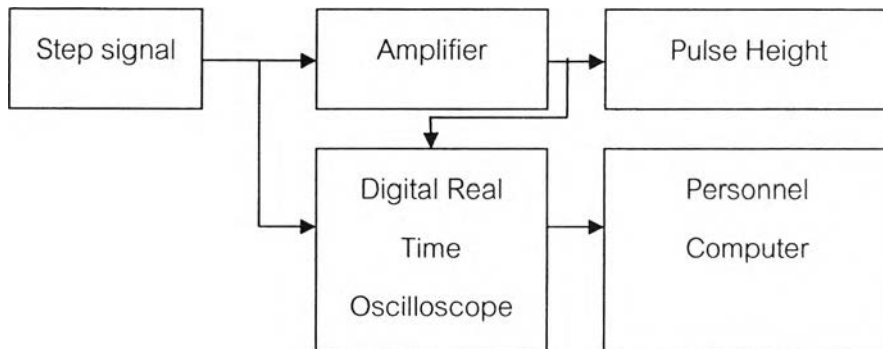


Fig. 4.5 System setup for the estimation of frequency response of spectroscopy amplifier.
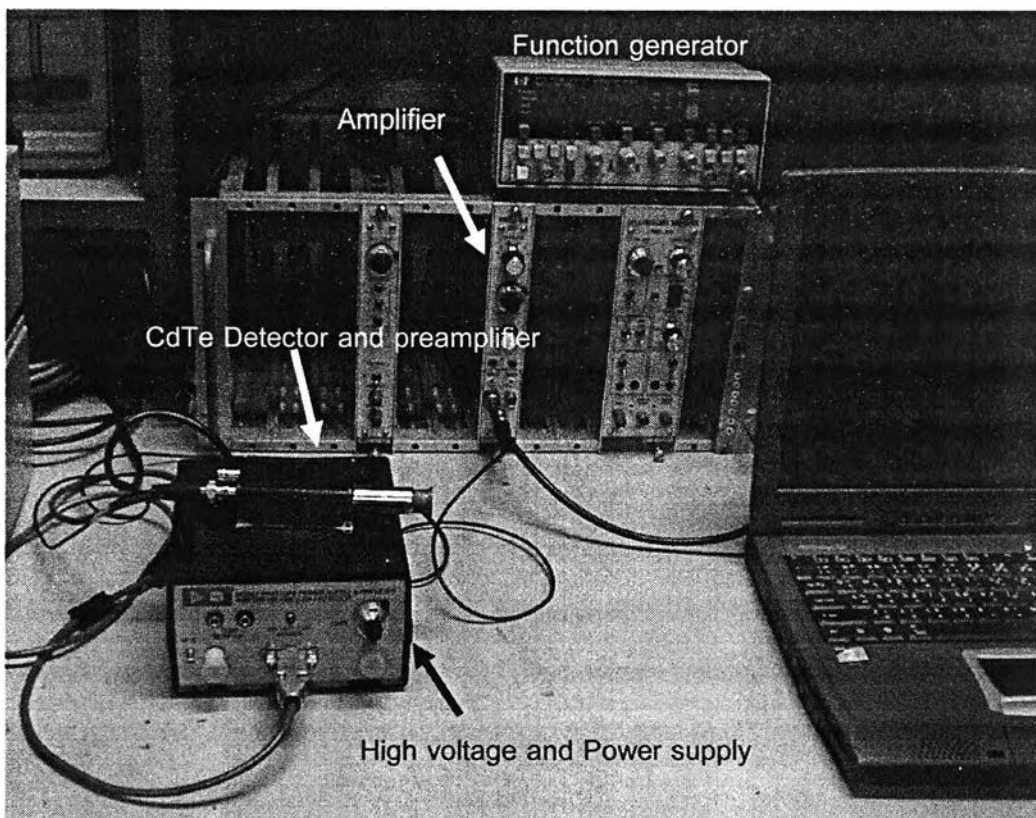


Fig. 4.6 Photograph of the set-up for the estimation of the frequency response of spectroscopy amplifier.

4.2.1.2.2 Digital filter design. The frequency response at each shaping time, obtained from the previous experiment (4.2.1.2.1), has to be transformed into a digital filter which has similar frequency response characteristics of a system under test. Those frequency responses are transformed into digital filters for the simulation of a time domain amplifier output by convolution method. The developed program for digital filter design is used to derive the filter kernel. The frequency response function after taken inverse discrete Fourier transform will change to time domain filter function; however the impulse response shape deviates considerably from the one under expectation. The improvement techniques i.e., truncating, shifting and windowing are applied to modify the impulse response giving almost similar filter function or the so-called final digital filter. The comparison of the final filter kernel's frequency response and the spectroscopy amplifier's frequency response at shaping time ranging from 0.5,1.0, 2.0, 4.0, 8.0 and 12.0 μs are shown in Fig.4.13 and Fig. 4.14 respectively.

4.2.2 Simulation for optimum shaping time searching. The input parameters prepared in previous experiment section are used for optimum shaping time searching. Front-end signal or detector-preamplifier which carries information of a complex noise and random consecutive pulses of mean counting rate at specific energy and pulse decay time constant is simulated. These simulated signals at a pulse rate of 50cps (pulser) 60 and 1000 cps of radiation count rate are taken to convolute with a final digital filter at shaping time of 0.5,1.0,2.0,4.0,8.0 and 12.0 μs for generating the spectroscopy amplifier output pulses. Fig. 4.16 show a convolution output of spectroscopy amplifier at shaping time of 0.5 μs and 12 μs. A distribution of those outputs is analyzed to perform the pulse height distribution in form of histogram for FWHM determination, as shown in Fig. 4.17. The plot of relation between shaping time and FWHM, with $2^{nd}$ order polynomial fitting which shows the optimum condition by simulation is shown in Fig. 4.18.

4.2.3 Manual check for optimum shaping time searching. The experimental equipment consists of the AMPTEK XTR100 CdTe low energy x-ray detector with preamplifier, high voltage biasing. CANBERRA 807 pulser, CANBERRA

2022 spectroscopy amplifier and CANBERRA 35 PLUS multichannel analyzer. A system set-up for optimum shaping time searching is shown in Fig. 4.7. The system is kept at a warm up time or half an hour to ensure their system stability. This system is set for x-ray spectrometer to analyze an energy resolution of 59.54 keV peak of Am-241 sources, which is related to the simulated amplifier output of previous experiment. The mean count rate from Am-241 source can be varied for the count rate of 60 and 1000 cps by varying a source to detector distance.

```
┌──────────┐     ┌──────────────┐     ┌──────────────┐     ┌──────────────────────┐
│ Detector │ ──> │ Preamplifier │ ──> │  Amplifier   │ ──> │ Pulse Height Analyzer│
│          │     │              │     │CANBERRA 2022 │     │  CANBERRA 35 PLUS    │
└──────────┘     └──────────────┘     └──────────────┘     └──────────────────────┘
     ▲      AMPTEK XTR100  ▲
┌──────────────┐     ┌──────────────┐
│ High Voltage │     │   Pulser     │
│              │     │ CANBERRA 807 │
└──────────────┘     └──────────────┘
```
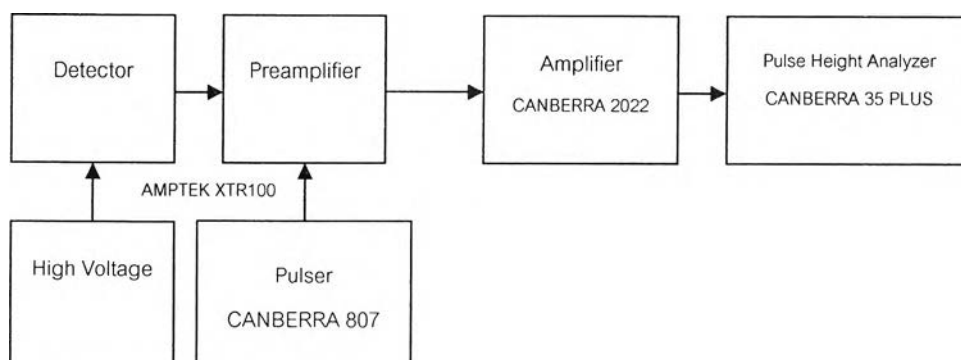
Fig.4.7 System setup for the energy resolution measurement.

The peak energy resolution of pulser at a count rate of 50 cps and Am-241 at 60 and 1000 cps of radiation count rate for shaping time settings from 0.5, 1.0, 2.0, 4.0, 8.0, and 12 μs are analyzed by a multichannel analyzer. Values of FWHM determined from energy peak resolutions are plot against shaping times after $2^{nd}$ order polynomial fitting. The plot shows the relation with clear as shown in Fig. 4.19.

## 4.3 Experimental results

### 4.3.1 Simulation of preamplifier noise.
The simulated noise waveform generated from empirical distribution function of sampled noise sequence is shown in Fig. 4.8a with mean, standard deviation and root mean square of 0.0036, 0.0012, 0.0021 volt, respectively. In agreement with those from measurement in the time domain found to be 0.0015, 0.0012, 0.0019 volt respectively. Fig.4.9 showed the similarity of power spectral densities of the measured and simulated noises. The later are calculated from sequence of noises from preamplifier output and simulation. Gaussian window is

selected to smooth the power spectral density curve and averaged by ten measurements and a hundred simulations. Even though, the statistical non-parametric test with two independent samples shows the dissimilarity between both power spectral densities. However, the equivalent noise charge (ENC) behavior after passing through a one order CR high-pass and third order low-pass Butterworth filter at the shaping time ranging from 0.25 to 12 µs shows the similarity between both measured noise from preamplifier and simulated noise, as shown in Fig. 4.10 and Fig. 4.11
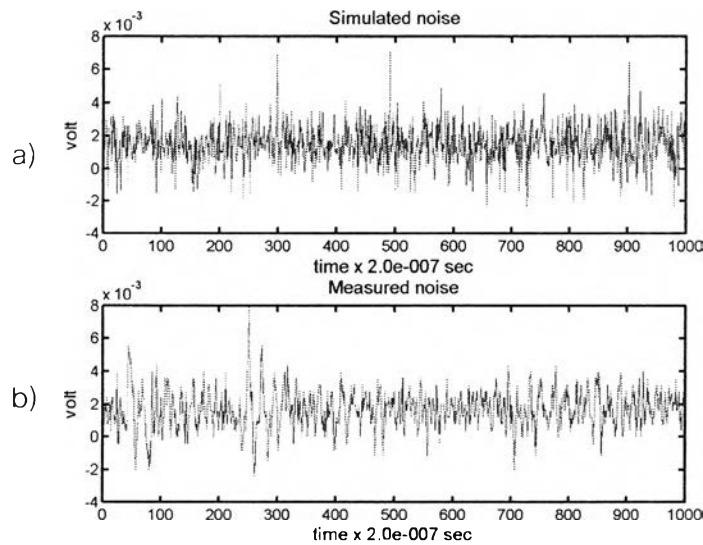


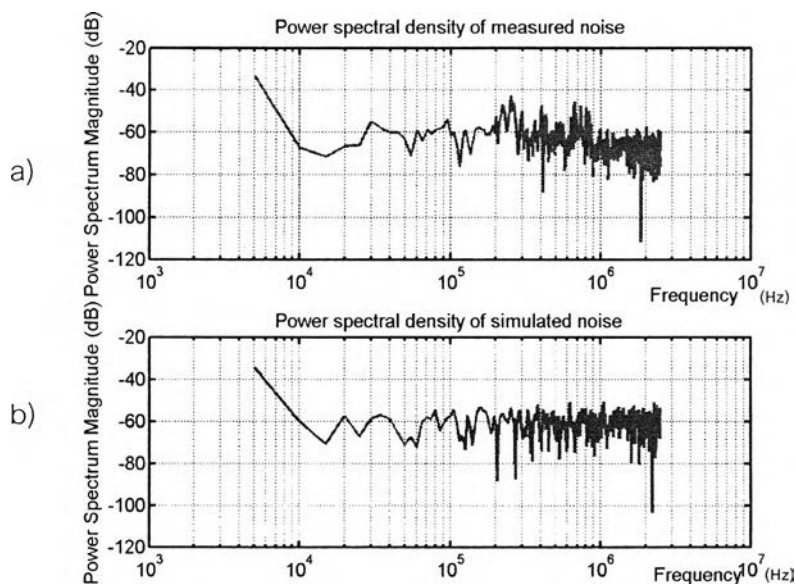Fig.4.8 a) Measured noise from preamplifier output b) Simulated noise waveform.



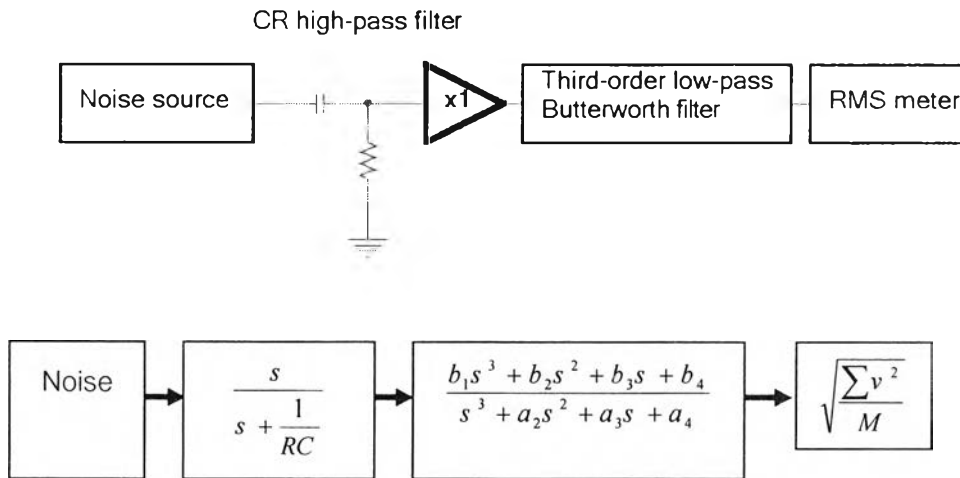Fig.4.9 Comparison of Power spectral densities of a) Measured and b) Simulated noise.

CR high-pass filter

```
┌─────────────┐        ┌──────────────────┐   ┌───────────┐
│ Noise source│──┤├──┬──│x1│ │Third-order low-pass│   │ RMS meter │
└─────────────┘     │     │Butterworth filter│   └───────────┘
                   ═╪═    └──────────────────┘
                    ⏚
```

```
┌────────┐   ┌──────────┐   ┌──────────────────────┐   ┌────────┐
│ Noise  │──▶│    s     │──▶│ b₁s³ + b₂s² + b₃s + b₄│──▶│ √ Σv²  │
│        │   │  ─────── │   │ ─────────────────────│   │   ─── │
│        │   │  s + 1   │   │  s³ + a₂s² + a₃s + a₄│   │    M   │
│        │   │     ──   │   │                      │   │        │
│        │   │     RC   │   │                      │   │        │
└────────┘   └──────────┘   └──────────────────────┘   └────────┘
```

$$\frac{s}{s + \dfrac{1}{RC}}$$

$$\frac{b_1 s^3 + b_2 s^2 + b_3 s + b_4}{s^3 + a_2 s^2 + a_3 s + a_4}$$

$$\sqrt{\frac{\sum v^2}{M}}$$

Fig. 4.10 The schematic of the numerical experiment test in noise behavior.
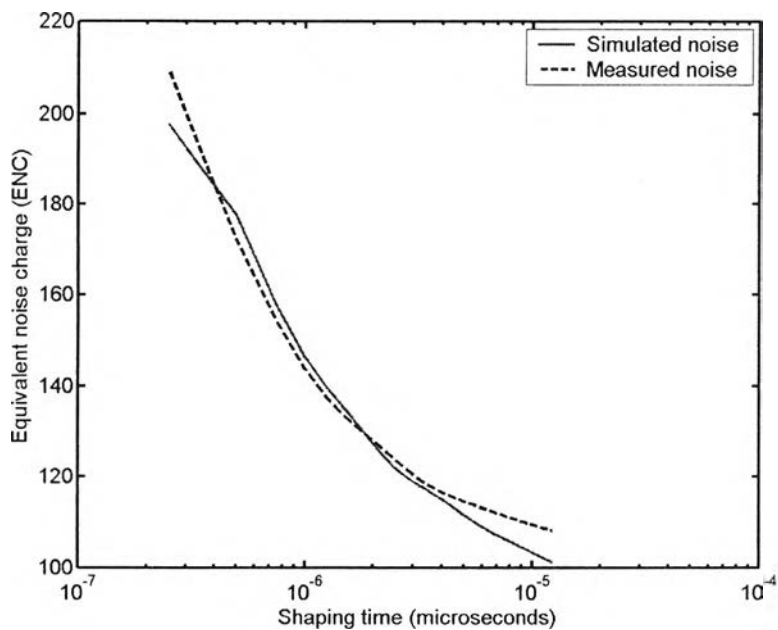


Fig. 4.11 The equivalent noise charge (ENC) of both measured and simulated noise.

**4.3.2 Simulation of front-end pulse output.** The front-end output or detector-preamplifier output is simulated with consideration of the pulse decay time and the time interval distribution as in equation (4.1) and (4.2). Thus the simulated pulse process the pulse height equivalent to photon energy, and other natural phenomenon like random photon emission in counting rate and the pulse decay time constant of the preamplifier. The generated pulse superimposed by simulated noise is used as detector-preamplifier output in optimum shaping time searching, as shown in Fig. 4.12.

At the same time, the generated pulse without noise added can be used as a simulated pulse pair, as shown in Fig. 4.13.
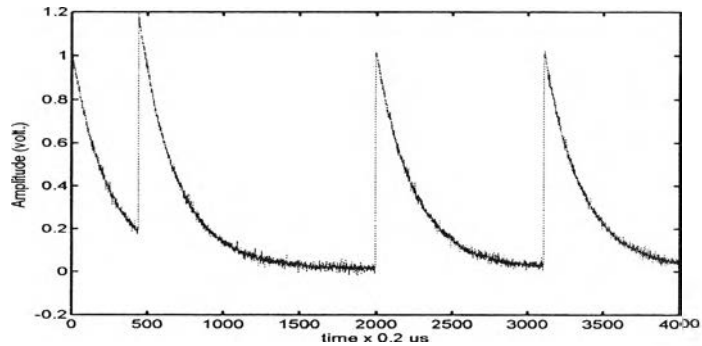


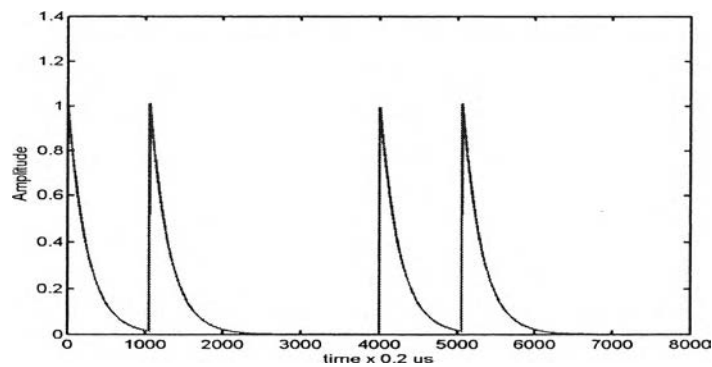Fig. 4.12 A simulated detector-preamplifier signal at specific energy.



Fig. 4.13 A simulated pulse pair output.

4.3.3 **Spectroscopy amplifier transfer function.** The calculated frequency responses at shaping time of 0.5, 1.0, 2.0, 4.0, 8.0 and 12.0 μs of spectroscopy amplifier are obtained. The frequency response of amplifier behaves like a band pass filter. The shortest shaping time constant (0.5 μs) has the corner frequency about 318.18 kHz with bandwidth about 200 kHz while the longest shaping time constant (12 μs) has the corner frequency about 13.26 kHz with band width about 10 kHz, as shown in Fig. 4.14. The slope of frequency response in the high pass section is less than that in the low pass section. The result agrees with the general spectroscopy amplifier design where the filter order of high pass section is less than the filter order of low pass section.

A noise like portion after the pass band arises from high frequency inaccuracy of simulation method.

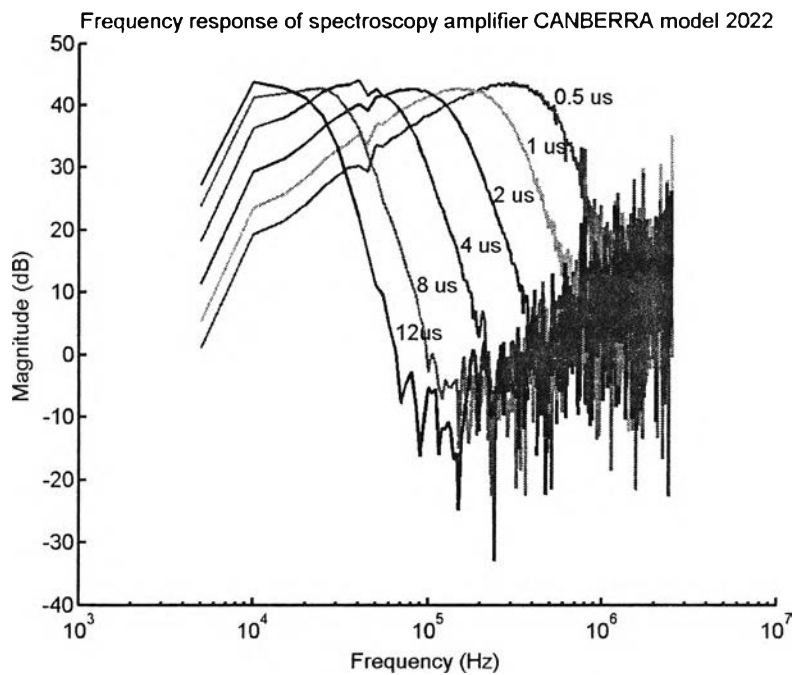Frequency response of spectroscopy amplifier CANBERRA model 2022

Fig. 4.14 Calculated frequency response of spectroscopy amplifier CANBERRA model 2022.
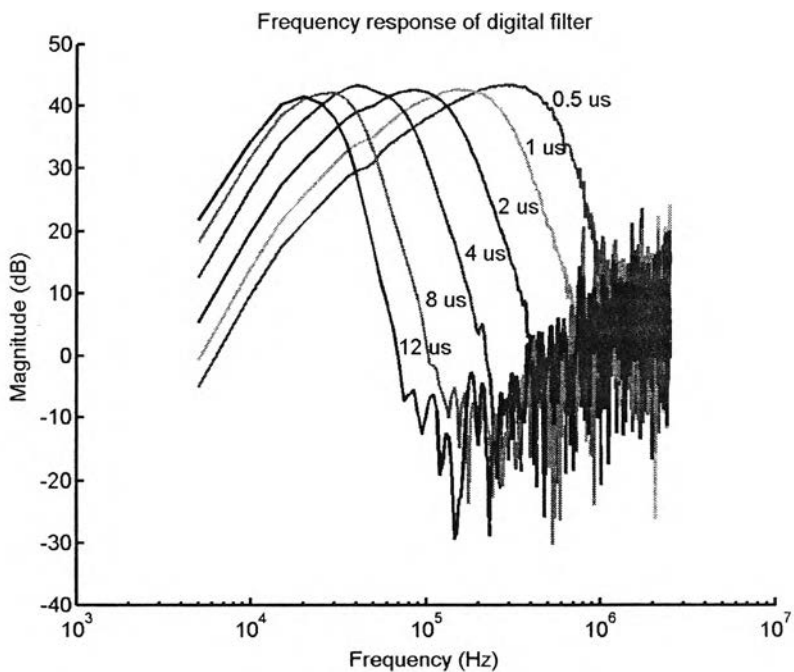
Fig. 4.15 Frequency response of digital filter equivalent to frequency response of spectroscopy amplifier CANBERRA model 2022.

**4.3.4 Digital filter design.** The digital filter, derived from the calculated frequency response of CANBERRA 2022 spectroscopy amplifier, is employed to perform as a wave shaper model at the shaping times of 0.5, 1.0, 2.0, 4.0, 8.0 and 12.0 µs. The digital filter design needs to be modified to fit frequency response of the amplifier by shifting, truncating and windowing. Filter kernels derived and modified in steps are shown in time domain, Fig. 4.16. They process the same frequency characteristics like the spectroscopy amplifier's frequency response in Fig. 4.14 and 4.15.
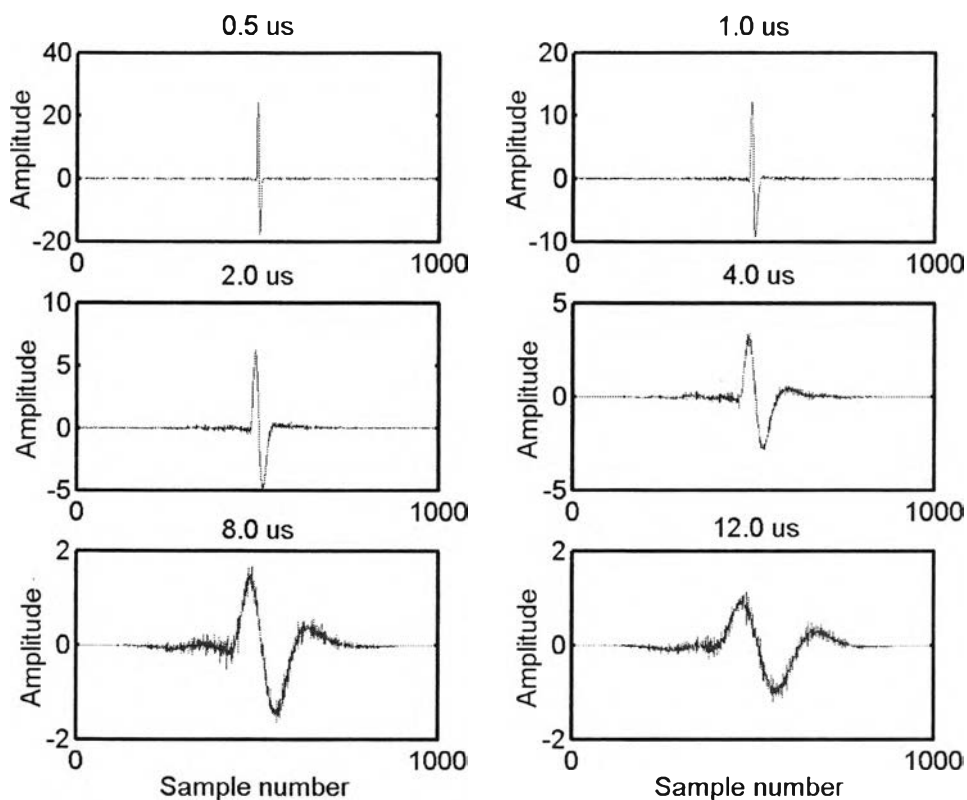


Fig. 4.16 The derived filter kernels which have the similar frequency response to spectroscopy amplifier under test.

The digital filter or filter kernels which is derived from frequency response of spectroscopy amplifier is used for pulse output generation in time domain simulation. Thereby a simulated front-end pulse signal is taken for convolution with digital filter at shaping time of 0.5 µs and 12 µs, resulting in an output pulse processing irregularities affecting pulse height fluctuation, as shown in Fig. 4.17.
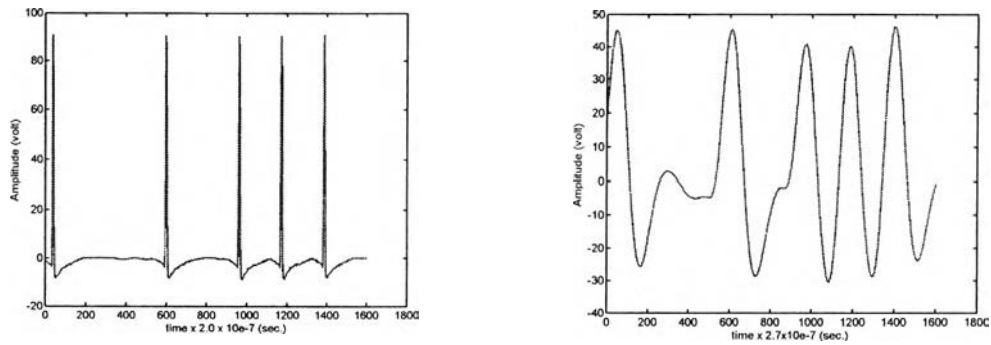
a) Without pileup (0.5 μs shaping time)        b) with pile up (12 μs shaping time)

Fig. 4.17 Amplifier output generated from convolution between front-end outputs and

filter kernel.

4.3.5 Simulation for optimum shaping time. The pulse height distribution in form of histogram or spectrum at peak energy of 59.54 keV and shaping time of 0.5 μs and 12 μs derived from simulation and conventional methods are compared, as shown in Fig. 4.18. In the simulation method, the fluctuation of signal due to a detector ($\sigma_1$ from 2.1.2) is not included. Therefore, the FWHM of peak obtained from both experiment and simulation are determined in term of a standard deviation per mean or peak resolution. The graphical plot of shaping time versus % peak resolution for optimum shaping time searching from both methods are shown in Fig. 4.19 and 4.20.



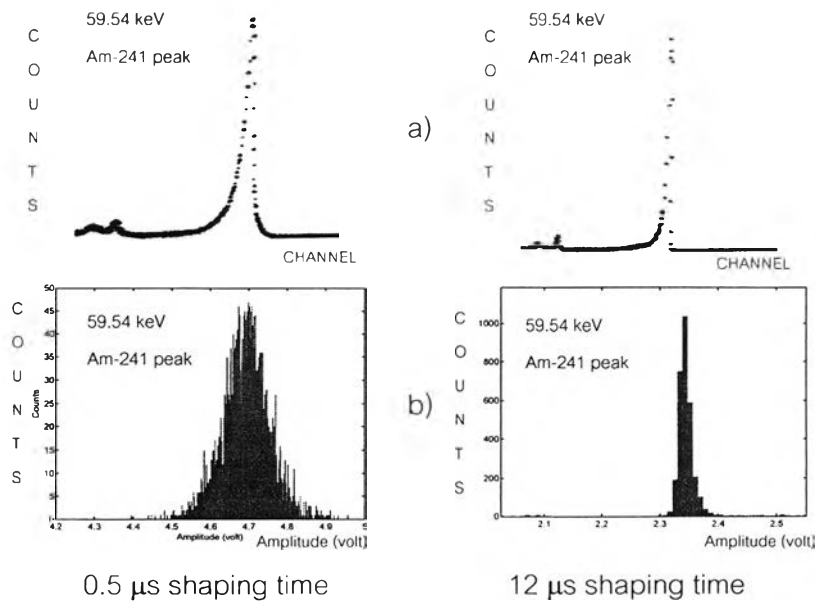0.5 μs shaping time                12 μs shaping time

Fig. 4.18 The FWHM resolution of system under test at 0.5 and 12 μs shaping time.
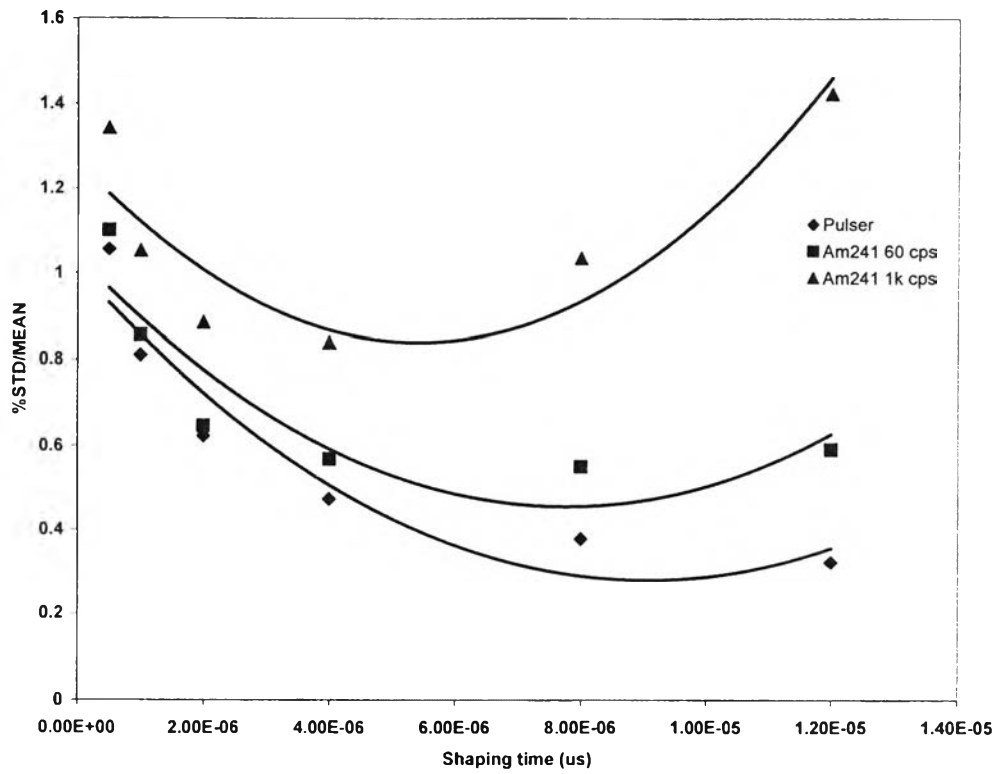
a) Conventional peak.   b) Simulation peak

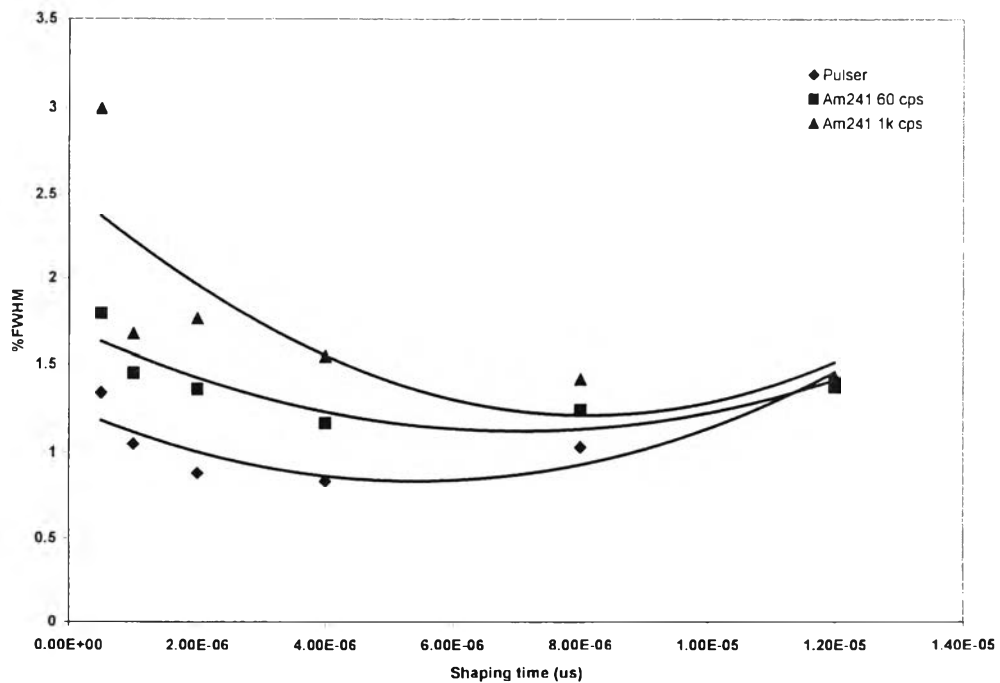Fig. 4.19 Graphical plot of optimum shaping time searching by simulation method.



Fig. 4.20 Graphical plot of optimum shaping time searching by manual check method.

The optimum shaping time to enhance the signal to noise ratio of the system under test is investigate at 50 cps generate from pulser, 60cps and 1 kcps from Am-241 γ-ray source with radiation detection. As show in fig. 4.19, the optimum shaping times from simulation technique for the source count rate of 50 cps from pulser, 60 and 1 kcps from Am-241 are 9.0, 8.0 and 5.7 μs, respectively while those obtained from manual searching, at the same source count rate in Fig. 4.20 yield the optimum shaping times at 5.0, 7.2 and 8.0 μs respectively. The discrepancies in optimum shaping times between these two searching methods are 80% at low count rate from pulse generator (50 cps), 11% at low count rate from x-ray source (60 cps) and 28.75 at high count rate from γ-ray source (1 kcps)